Journal of Computational Physics: X 7 (2020) 100060

Contents lists available at ScienceDirect

Journal of Computational Physics: X

www.elsevier.com/locate/jcpx

Height-function curvature estimation with arbitrary order on non-uniform Cartesian grids

Fabien Evrard *, Fabian Denner, Berend van Wachem

Lehrstuhl für Mechanische Verfahrenstechnik, Otto-von-Guericke-Universität Magdeburg, Universitätsplatz 2, 39106 Magdeburg, Germany

ARTICLE INFO

Article history:
Received 18 November 2019
Received in revised form 6 April 2020
Accepted 18 May 2020
Available online 22 May 2020

Keywords:
Curvature
Volume-of-fluid
Height-function
Non-uniform grid
Arbitrary order

ABSTRACT

This paper proposes a height-function algorithm to estimate the curvature of two-dimensional curves and three-dimensional surfaces that are defined implicitly on two- and three-dimensional non-uniform Cartesian grids. It relies on the reconstruction of local heights, onto which polynomial height-functions are fitted. The algorithm produces curvature estimates of order $N-1$ anywhere in a stencil of $(N+1)^{d-1}$ heights computed from the volume-fraction data available on a d-dimensional non-uniform Cartesian grid. These estimates are of order N at the centre of the stencil when it is symmetric about its main axis. This is confirmed by a comprehensive convergence analysis conducted on the errors associated with the application of the algorithm to a fabricated test-curve and test-surface.

1. Introduction

When modelling interfacial flows, accurately estimating the curvature of the fluid-fluid interface is key to correctly account for capillary effects, and to avoid the generation of parasitic flow currents [1–3]. In the context of the widely used *volume-of-fluid* (VOF) method [4–8], the immiscible fluid phases a and b are identified by the indicator function

$$\chi(\boldsymbol{x}) = \begin{cases} 1 & \text{if } \boldsymbol{x} \in \text{fluid } a \\ 0 & \text{if } \boldsymbol{x} \in \text{fluid } b \end{cases} . \tag{1}$$

The quantity that is correspondingly available in each cell K of the computational grid is the local volume-fraction

$$\gamma_K = \frac{1}{\ell(K)} \int_K \chi(\boldsymbol{x}) \, \mathrm{d}\boldsymbol{x}, \tag{2}$$

where $\ell(K) = \int_K \mathrm{d}\boldsymbol{x}$ is the Lebesgue measure of K. The interface between the domains occupied by fluid a and fluid b can be represented in the form of an implicit hypersurface $F(\boldsymbol{x}) = 0$, resulting in the local mean curvature of this interface reading as [9][1]

* Corresponding author.
E-mail address: fabien.evrard@ovgu.de (F. Evrard).

[1] Note that Eq. (3) is applicable to both the two- and three-dimensional cases because the following definition of the three-dimensional mean curvature is considered in the present work: $\kappa = \kappa_1 + \kappa_2$, κ_1 and κ_2 being the principal curvatures of the surface. Goldman [9] uses the following definition: $\kappa = (\kappa_1 + \kappa_2)/2$ for the three-dimensional mean curvature, yielding formulas for the two- and three-dimensional cases that differ by a factor 2.

https://doi.org/10.1016/j.jcpx.2020.100060

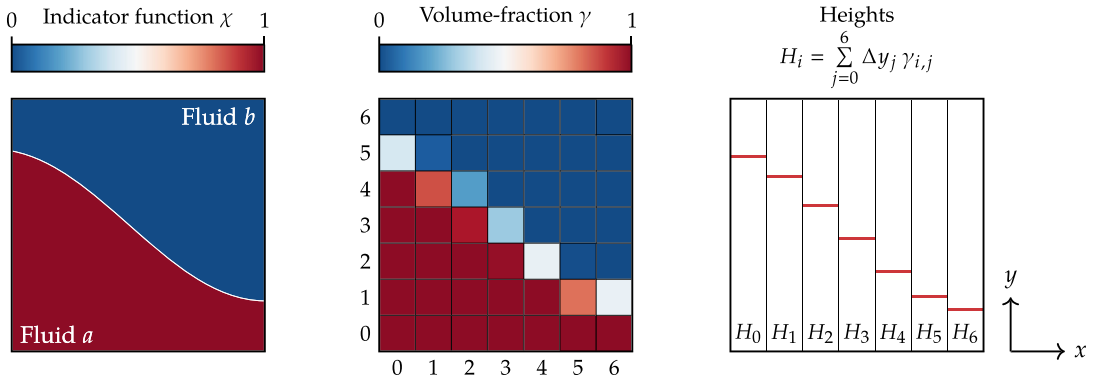

Fig. 1. Illustration of the computation of the heights of fluid associated with an interface, in the context of the VOF method. The left figure shows the indicator function for the fluid phases a and b. The central figure shows the associated volume-fraction field on a 7×7 uniform Cartesian grid. The right figure shows the corresponding heights of fluid, if the y-direction is chosen to be the "vertical" direction, *i.e.* the direction of summation of the volume-fractions.

$$\kappa = \frac{\nabla F^{\mathrm{T}} \cdot \nabla \left(\nabla F \right) \cdot \nabla F - |\nabla F|^2 \, \mathrm{tr} \left(\nabla \left(\nabla F \right) \right)}{|\nabla F|^3} \, . \tag{3}$$

The challenge in estimating κ thus lies in the estimation of the first and second partial derivatives of the function $F(\boldsymbol{x})$ at the location of the interface, from the values of the integrals of χ in the computational cells. This has been addressed in numerous ways and with varying success in the literature, yet the only method that has been shown to converge with mesh refinement is the *height-function* (HF) method [10–15]. The HF method relies on the computation of local *heights of fluid*, which are then used to compute the first and second partial derivatives of the interface. Having chosen a local "vertical" direction (based on the components of the local interface normal vector), these heights are simply obtained from the summation of the volume-fractions along the vertical direction, as illustrated in Fig. 1. The formulation of the HF method classically found in the literature is second-order accurate and restricted to uniform Cartesian grids [10,11,13,3]. A strategy to extend the HF method to higher orders was first suggested by Sussman and Ohta [12], and applied to obtain fourth-order accurate estimates of curvature on three-dimensional uniform Cartesian grids. Francois and Swartz [16] and Bornia et al. [17] then proposed fourth-order formulas for the two-dimensional case, with Francois and Swartz [16] considering two-dimensional non-uniform Cartesian grids. More recently, Zhang [18] extended the HF method to arbitrary order on two-dimensional uniform Cartesian grids.

To this date, however, there does not exist a unique, arbitrary-order, HF method that allows to estimate curvature on two- and three-dimensional non-uniform Cartesian grids. In this paper, we present such a method for the estimation of curvature on two- and three-dimensional non-uniform Cartesian grids, with arbitrary order of accuracy. Moreover, we show that the proposed method allows to estimate curvature anywhere in the stencil of heights, *i.e.* not necessarily at its centre, and that the said stencil does not need to be made of contiguous intervals. Section 2 and 3 present the proposed approach for the two- and three-dimensional cases, respectively. These are then validated in Section 4, where they are shown to produce arbitrarily accurate estimates of curvature on non-uniform Cartesian grids, at any location of the column stencil. Finally, conclusions are drawn in Section 5. Note that a list of low-order formulas for the two- and three-dimensional cases, and the C implementations of the approaches presented in Section 2 and 3, are provided in the appendix.

2. Two-dimensional case

Consider an arbitrary two-dimensional curve that can locally be expressed in the form of the height-function

$$z = f(x) \, , \tag{4}$$

as illustrated in Fig. 2. To each local interval $[x_i, x_{i+1}]$, we can associate the *height*

$$H_i = \frac{1}{\Delta x_i} \int_{x_i}^{x_{i+1}} f(x) \, \mathrm{d}x \, , \tag{5}$$

where $\Delta x_i = x_{i+1} - x_i$. The middle of this interval is defined as $x_{i+1/2} = (x_{i+1} + x_i)/2$. In many scientific fields – such as interfacial flow modelling – the heights H_i constitute one of the few pieces of information that are available to recover important geometric properties of the curve (*e.g.* normals, curvatures). Without loss of generality, let us now consider the interval $[x_0, x_1]$ centred around the value $x_{1/2}$, which is fixed. We choose the interval to be such that $\Delta x_0 = h$, with $h \in \mathbb{R}_+$, and we assume that all intervals $[x_i, x_{i+1}]$, with $i \in \mathbb{Z}$, are such that $\Delta x_i = \alpha_i \, h$ where $\alpha_i \in \mathbb{R}_+$ is a constant. This way, by

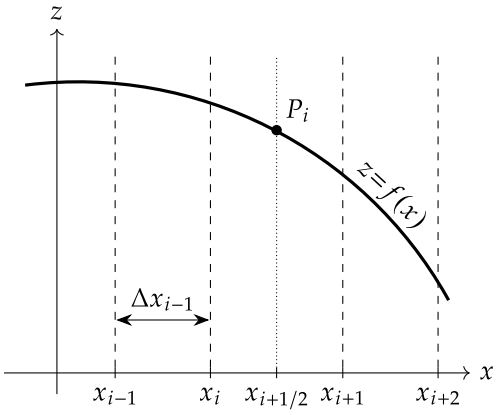

Fig. 2. An arbitrary curve, locally defined as $z = f(x)$. The middle of the interval $[x_i, x_{i+1}]$ is $x_{i+1/2}$. The point P_i is located on the curve at $(x_{i+1/2}, f(x_{i+1/2}))$.

varying the value of h while keeping everything else constant, we can stretch the stencil of intervals (or *columns*) centred around $[x_0, x_1]$ without modifying the ratio between their widths. It is known that when $\Delta x_{-1} = \Delta x_0 = \Delta x_1 = h$, *i.e.* when the three consecutive columns centred around $x_{1/2}$ are of uniform width, then κ, the curvature of the curve at point $P_0 = (x_{1/2}, f(x_{1/2}))$, is given by [10,17]

$$\kappa = \frac{H_{xx}}{\left(H_x^2 + 1\right)^{3/2}} + O\left(h^2\right), \tag{6}$$

with H_x and H_{xx} obtained from the central-difference formulas

$$H_x = \frac{H_1 - H_{-1}}{2h}, \tag{7a}$$

$$H_{xx} = \frac{H_1 - 2\,H_0 + H_1}{h^2}. \tag{7b}$$

In fact, this process can be shown to be equivalent to finding the coefficients a, b, and c of the parabola

$$\tilde{f}(x) = ax^2 + bx + c, \tag{8}$$

that satisfy

$$H_i = \frac{1}{\Delta x_i} \int_{x_i}^{x_{i+1}} \tilde{f}(x)\,\mathrm{d}x, \quad \forall i \in \{-1, 0, 1\}, \tag{9}$$

the curvature κ thus being equivalently given by [19]

$$\kappa = \frac{\tilde{f}_{xx}(x_{1/2})}{\left(\tilde{f}_x(x_{1/2})^2 + 1\right)^{3/2}} + O\left(h^2\right). \tag{10}$$

We now extend this analogy to arbitrary order, and to non-uniform column widths. Consider the polynomial function of order N

$$\tilde{f}(x) = \mathbf{A}^{\mathrm{T}}\mathbf{P}(x), \tag{11}$$

where $\mathbf{A}$ is a vector of $N+1$ scalar coefficients, and $\mathbf{P}(x)$ the vector of polynomial basis functions

$$P_j(x) = x^{j-1},\ j \in \{1, \ldots, N+1\}. \tag{12}$$

The heights generated by the function $\tilde{f}$ read as

$$\tilde{H}_i = \frac{1}{\Delta x_i} \int_{x_i}^{x_{i+1}} \mathbf{A}^{\mathrm{T}}\mathbf{P}(x)\,\mathrm{d}x = \frac{1}{\Delta x_i}\mathbf{A}^{\mathrm{T}}\left(\mathbf{Q}(x_{i+1}) - \mathbf{Q}(x_i)\right), \tag{13}$$

where $\mathbf{Q}(x)$ is the vector of antiderivatives of the basis functions in $\mathbf{P}(x)$, that is

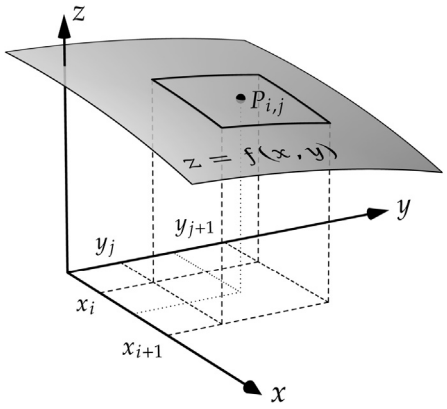

Fig. 3. An arbitrary surface, locally defined as $z = f(x, y)$. The point $P_{i,j}$ is located on the surface at $(x_{i+1/2}, y_{j+1/2}, f(x_{i+1/2}, y_{j+1/2}))$.

$$Q_j(x) = \frac{x^j}{j},\ j \in \{1, \ldots, N+1\}\,. \tag{14}$$

Assuming that $N+1$ heights are available as inputs, each being associated to an arbitrary interval $[x_k, x_{k+1}]$ with $k \in \mathbb{Z}$ (the intervals not needing to be consecutive), then equating these heights to those generated by the function $\tilde{f}$ reduces to solving the following linear system for $\mathbf{A}$,

$$\mathbf{MA} = \mathbf{H}\,, \tag{15}$$

where $\mathbf{H}$ is a vector containing the $N+1$ heights. Each ith row of the matrix $\mathbf{M}$ reads as

$$M_{i,j} = \frac{Q_j(x_{k+1}) - Q_j(x_k)}{\Delta x_k},\ j \in \{1, \ldots, N+1\}\,, \tag{16}$$

where $[x_k, x_{k+1}]$ is the arbitrary interval associated with the ith height in $\mathbf{H}$. The first and second derivatives of the polynomial $\tilde{f}(x)$ can be expressed at any coordinate x as a function of the scalar coefficients in $\mathbf{A}$. When $x = 0$, however, these first and second derivatives are each a function of only one scalar coefficient of $\mathbf{A}$. Since we want to estimate curvature at $x = x_{1/2}$, then it is judicious to express the limits of the intervals $[x_k, x_{k+1}]$ in terms of their value relative to $x_{1/2}$ when calculating the coefficients of the matrix $\mathbf{M}$, *i.e.* to locate the origin of the local reference frame at $x = x_{1/2}$. This way, the first and second derivatives of $\tilde{f}$ at $x = x_{1/2}$ are simply given by

$$\tilde{f}_x(0) = A_2\,, \tag{17a}$$

$$\tilde{f}_{xx}(0) = 2\,A_3\,, \tag{17b}$$

so the curvature of the curve at point $P_0 = (x_{1/2}, f(x_{1/2}))$ is given by [9]

$$\kappa = \frac{2\,A_3}{\left(A_2^2 + 1\right)^{3/2}} + O\left(h^{N-1}\right)\,, \tag{18}$$

meaning that $\kappa = 2\,A_3/(A_2^2+1)^{3/2}$ is an approximation of the curvature at P_0 of order $N-1$. If the stencil of $N+1$ height intervals is symmetric about the value $x = x_{1/2}$ and includes the interval $[x_0, x_1]$, then the approximation in Eq. (18) can be shown to be of order N [16,18].

The first and second derivatives obtained with this approach, in the central and boundary cells of a stencil of $N+1$ consecutive intervals of uniform width, are listed in Appendix A.1 for values of N up to 4. The C code allowing to estimate curvature at any coordinate x_c from $N+1$ heights is given in Appendix B.1.

3. Three-dimensional case

Consider an arbitrary surface that can locally be expressed in the form of the height-function

$$z = f(x, y)\,, \tag{19}$$

as illustrated in Fig. 3. To each local domain $[x_i, x_{i+1}] \times [y_j, y_{j+1}]$, we can associate the *height*

$$H_{i,j} = \frac{1}{\Delta x_i\,\Delta y_j} \int_{x_i}^{x_{i+1}} \int_{y_j}^{y_{j+1}} f(x, y)\,\mathrm{d}x\,\mathrm{d}y\,, \tag{20}$$

where $\Delta x_i = x_{i+1} - x_i$ and $\Delta y_j = y_{j+1} - y_j$. The centre of this domain is defined as $(x_{i+1/2}, y_{j+1/2}) = ((x_i + x_{i+1})/2, (y_j + y_{j+1})/2)$. Without loss of generality, let us consider the domain $[x_0, x_1] \times [y_0, y_1]$ centred around the point $(x_{1/2}, y_{1/2})$, which is fixed. We choose the domain to be such that $\Delta x_0 = h$ and $\Delta y_0 = rh$, with $(h, r) \in \mathbb{R}_+^2$, and we assume that all intervals $[x_i, x_{i+1}]$ and $[y_j, y_{j+1}]$, with $(i, j) \in \mathbb{Z}^2$, are such that $\Delta x_i = \alpha_i h$ and $\Delta y_j = \beta_j rh$, where $(\alpha_i, \beta_j) \in \mathbb{R}_+^2$ are constants. This way, by varying the value of h while keeping everything else constant, we can stretch the stencil of columns centred around $[x_0, x_1] \times [y_0, y_1]$ without modifying the ratio between their widths. It is known that when $\Delta x_{-1} = \Delta x_0 = \Delta x_1 = h$ and $\Delta y_{-1} = \Delta y_0 = \Delta y_1 = rh$, then κ, the mean curvature of the surface at point $P_{0,0} = (x_{1/2}, y_{1/2}, f(x_{1/2}, y_{1/2}))$, is given by [11]

$$\kappa = \frac{H_{xx}\left(1 + H_y^2\right) + H_{yy}\left(1 + H_x^2\right) - 2\,H_x\,H_y\,H_{xy}}{\left(H_x^2 + H_y^2 + 1\right)^{3/2}} + O\left(h^2\right), \tag{21}$$

with H_x, H_y, H_{xx}, H_{yy}, and H_{xy} obtained from the central-difference formulas

$$H_x = \frac{H_{1,0} - H_{-1,0}}{2h}, \tag{22a}$$

$$H_y = \frac{H_{0,1} - H_{0,-1}}{2rh}, \tag{22b}$$

$$H_{xx} = \frac{H_{1,0} - 2\,H_{0,0} + H_{1,0}}{h^2}, \tag{22c}$$

$$H_{yy} = \frac{H_{0,1} - 2\,H_{0,0} + H_{0,1}}{(rh)^2}, \tag{22d}$$

$$H_{xy} = \frac{H_{1,1} + H_{-1,-1} - H_{1,-1} - H_{-1,1}}{4rh^2}. \tag{22e}$$

Let us now extend the strategy employed for the two-dimensional case to the three-dimensional case. To that end, consider the bivariate polynomial function

$$\tilde{f}(x, y) = \mathbf{A}^{\mathrm{T}} \mathrm{vec}\left(\mathbf{P}(x)\,\mathbf{P}(y)^{\mathrm{T}}\right), \tag{23}$$

where $\mathbf{A}$ is a vector of $(N+1) \times (N+1)$ scalar coefficients, and $\mathrm{vec}\left(\mathbf{P}(x)\,\mathbf{P}(y)^{\mathrm{T}}\right)$ the vector of $(N+1) \times (N+1)$ bivariate polynomial basis functions, which consists of the concatenation of the columns of the matrix formed by the outer product of $\mathbf{P}(x)$ by $\mathbf{P}(y)$. The heights generated by the function $\tilde{f}$ read as

$$\begin{aligned} \tilde{H}_{i,j} &= \frac{1}{\Delta x_i\,\Delta y_j} \int_{x_i}^{x_{i+1}} \int_{y_j}^{y_{j+1}} \mathbf{A}^{\mathrm{T}} \mathrm{vec}\left(\mathbf{P}(x)\,\mathbf{P}(y)^{\mathrm{T}}\right) \mathrm{d}x\,\mathrm{d}y \\ &= \frac{1}{\Delta x_i\,\Delta y_j} \mathbf{A}^{\mathrm{T}} \mathrm{vec}\left(\left(\mathbf{Q}(x_{i+1}) - \mathbf{Q}(x_i)\right)\left(\mathbf{Q}(y_{j+1}) - \mathbf{Q}(y_j)\right)^{\mathrm{T}}\right) \end{aligned} \tag{24}$$

where $\mathbf{Q}(x)$ is the vector of $N+1$ antiderivatives defined in Eq. (14). Assume that $(N+1) \times (N+1)$ heights, associated to $N+1$ arbitrary intervals $[x_k, x_{k+1}]$ and $N+1$ arbitrary intervals $[y_l, y_{l+1}]$, with $(k, l) \in \mathbb{Z}^2$, are available as inputs. Equating these heights to those generated by the function $\tilde{f}$ then reduces to solving the following linear system for $\mathbf{A}$,

$$\mathbf{M}\mathbf{A} = \mathbf{H}, \tag{25}$$

where $\mathbf{H}$ is a vector containing the $(N+1) \times (N+1)$ heights. Each ith row of the matrix $\mathbf{M}$ reads as

$$M_{i,j} = \frac{\left(Q_m(x_{k+1}) - Q_m(x_k)\right)\left(Q_n(y_{l+1}) - Q_n(y_l)\right)}{\Delta x_k\,\Delta y_l}, \quad \begin{cases} n = 1 + \lfloor (j-1)/(N+1) \rfloor \\ m = j - (n-1)(N+1) \end{cases}, \quad j \in \{1, \ldots, (N+1)^2\}, \tag{26}$$

where $[x_k, x_{k+1}]$ and $[y_l, y_{l+1}]$ are the arbitrary intervals forming the domain associated with the ith height in $\mathbf{H}$. The first and second partial derivatives of the bivariate polynomial $\tilde{f}(x, y)$ can be expressed at any coordinate (x, y) as a function of the scalar coefficients in $\mathbf{A}$. When $x = y = 0$, however, these first and second partial derivatives are each a function of only one scalar coefficient of $\mathbf{A}$. Since we want to estimate curvature at $(x, y) = (x_{1/2}, y_{1/2})$, then it is judicious to express the limits of the intervals $[x_k, x_{k+1}]$ and $[y_l, y_{l+1}]$ in terms of their value relative to $x_{1/2}$ and $y_{1/2}$, respectively, when calculating the coefficients of the matrix $\mathbf{M}$, *i.e.* to locate the origin of the local reference frame at $(x, y) = (x_{1/2}, y_{1/2})$. This way, the first and second partial derivatives of $\tilde{f}$ at $(x, y) = (x_{1/2}, y_{1/2})$ are simply given by

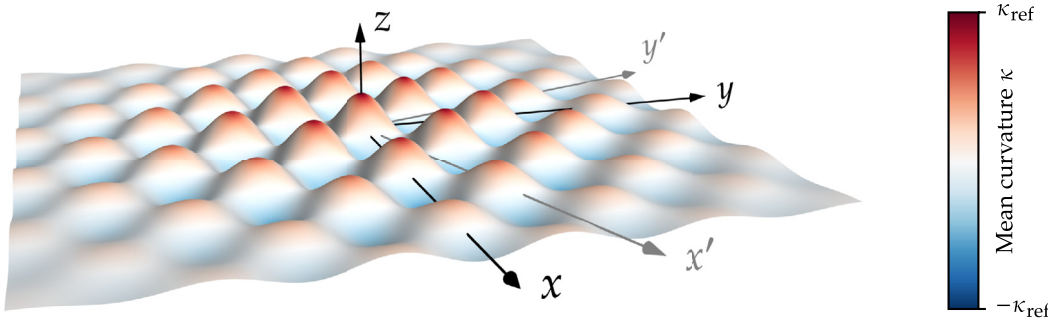

Fig. 4. Test-surface given by Eq. (29) with $\lambda = \eta$, coloured based on the local mean curvature normalised by its maximum value κ_{ref}.

$$\tilde{f}_x(0,0) = A_2\,, \tag{27a}$$
$$\tilde{f}_y(0,0) = A_{N+2}\,, \tag{27b}$$
$$\tilde{f}_{xx}(0,0) = 2\,A_3\,, \tag{27c}$$
$$\tilde{f}_{yy}(0,0) = 2\,A_{2N+3}\,, \tag{27d}$$
$$\tilde{f}_{xy}(0,0) = A_{N+3}\,, \tag{27e}$$

so the mean curvature of the surface at point $P_{0,0} = (x_{1/2}, y_{1/2}, f(x_{1/2}, y_{1/2}))$ is given by [9]

$$\kappa = \frac{2\left(A_3\left(1+A_{N+2}^2\right) + A_{2N+3}\left(1+A_2^2\right) - A_2\,A_{N+2}\,A_{N+3}\right)}{\left(A_2^2 + A_{N+2}^2 + 1\right)^{3/2}} + O\left(h^{N-1}\right). \tag{28}$$

If the stencil of $(N+1)\times(N+1)$ height domains is symmetric about the axis $x = x_{1/2}$ and $y = y_{1/2}$, and includes the intervals $[x_0, x_1]$ and $[y_0, y_1]$, then the previous approximation can be shown to be of order N.

The first and second partial derivatives obtained with this approach, in the central and boundary cells of a stencil formed by $N+1$ consecutive intervals of uniform width along both x- and y-axis, are listed in Appendix A.2 for values of N up to 4. The C code allowing to estimate curvature at any coordinate (x_c, y_c) from $(N+1)\times(N+1)$ heights is given in Appendix B.2.

4. Numerical tests

In order to test the proposed approach for curvature estimation, let us consider the surface

$$z = \frac{\lambda}{4}\cos\left(\frac{2\pi\,x}{\lambda}\right)\cos\left(\frac{2\pi\,y}{\eta}\right)\exp\left(-\frac{x^2}{4\lambda^2}\right)\exp\left(-\frac{y^2}{4\eta^2}\right), \tag{29}$$

which cannot be rewritten in the form of a polynomial height-function of finite order. This test-surface is illustrated in Fig. 4. To prevent the systematic occurrence of cases where the principal directions of curvature of the surface are aligned with the x- and y-axis, we conduct our tests in a reference frame $\mathcal{R}' = (x', y', z)$ that results from the rotation of the fundamental reference frame $\mathcal{R} = (x, y, z)$ about the z-axis, with a random angle $\theta \in [0, 2\pi]$. We consider the following domains for the two- and three-dimensional studies, namely $\mathcal{D}_{2\text{d}} = \{x' \in \mathbb{R} \mid 0 \le x' \le \lambda\}$ and $\mathcal{D}_{3\text{d}} = \{(x', y') \in \mathbb{R}^2 \mid 0 \le x' \le \lambda \text{ and } 0 \le y' \le \lambda\}$, respectively. The study of the two-dimensional curvature estimation is conducted in the (x', z) plane, and the test-curve thus corresponds to the intersection of the test-surface with the (x', z) plane. The test-curve and test-surface respectively associated with the domains $\mathcal{D}_{2\text{d}}$ and $\mathcal{D}_{3\text{d}}$ are illustrated in Fig. 5, where the test-curve used for the two-dimensional study is highlighted in red, and the test-surface used for the three-dimensional study is coloured based on its mean curvature.

4.1. Two- and three-dimensional convergence studies

Figs. 6 and 7 show the errors associated with the estimation of curvature for the two- and three-dimensional cases, respectively. Four different types of stencils are considered in each study, corresponding to the four columns of graphs of each figure. Curvature is estimated at the centre of the stencil, but also in cells that lie on its boundary.

For the two-dimensional study (Fig. 6), the following types of stencils are considered:

- *A* Symmetric stencil of $N+1$ consecutive intervals of uniform width along the x'-axis.
- *B* Symmetric stencil of $N+1$ consecutive intervals of non-uniform width along the x'-axis (the intervals are stretched by a factor $s = 1.2$ around the central interval).

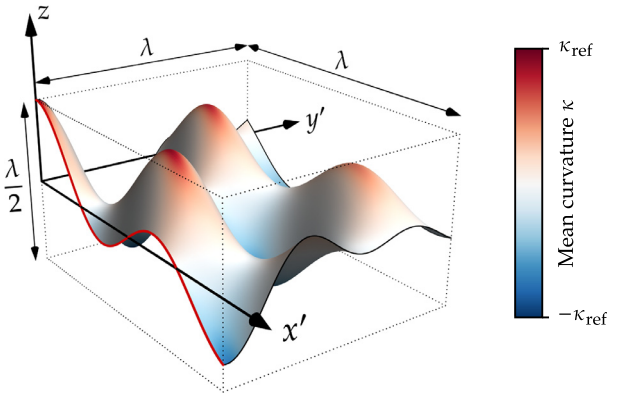

Fig. 5. Test-surface and test-curve associated with the test-domains $\mathcal{D}_{2d}$ and $\mathcal{D}_{3d}$ considered for the two- and three-dimensional studies, with $\lambda = 1$, $\eta = 2/3$, and $\theta = \pi/10$. The test-surface used for the three-dimensional study is coloured based on its mean curvature normalised by its maximum value κ_{ref}, and the test-curve used for the two-dimensional study in the (x', z) plane is highlighted in red.

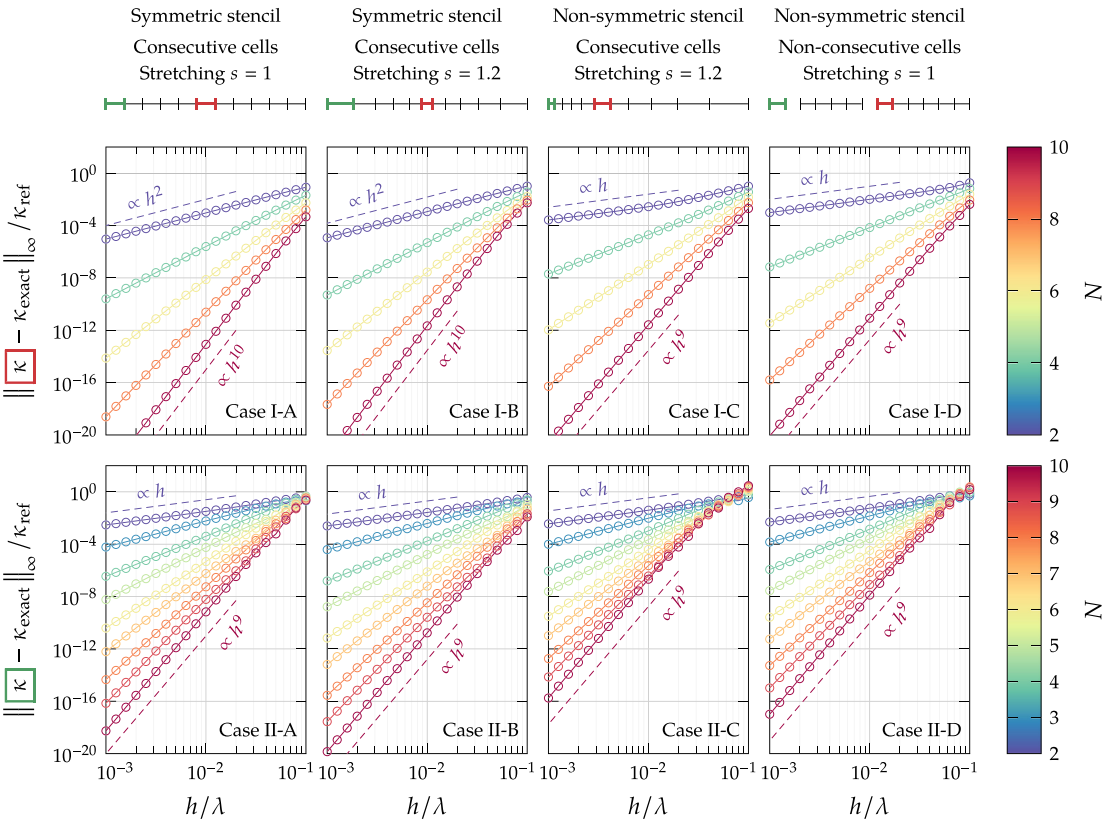

Fig. 6. Maximum errors associated with estimating the curvature of the test-curve in $N_S = 5 \times 10^5$ random configurations. Four different stencil types are considered, each corresponding to a column of the figure. The stencils are sketched at the top of the columns. The first row of graphs corresponds to the errors obtained in the central cell of the stencil, and the second row to the errors obtained in the left cell of the stencil. The use of $N+1$ heights results in a curvature estimate of order $N-1$, unless the stencil is symmetric about its centre, in which case curvature can be estimated at its centre with order N.

C Non-symmetric stencil of $N+1$ consecutive intervals of non-uniform width along the x'-axis (the intervals are stretched by a factor $s = 1.2$ in the positive x' direction).
D Non-symmetric stencil of $N+1$ non-consecutive intervals of uniform width along the x'-axis.

Curvature (and the associated error) is computed in:

I The central interval of the stencil (for N even).
II The extreme left interval of the stencil.

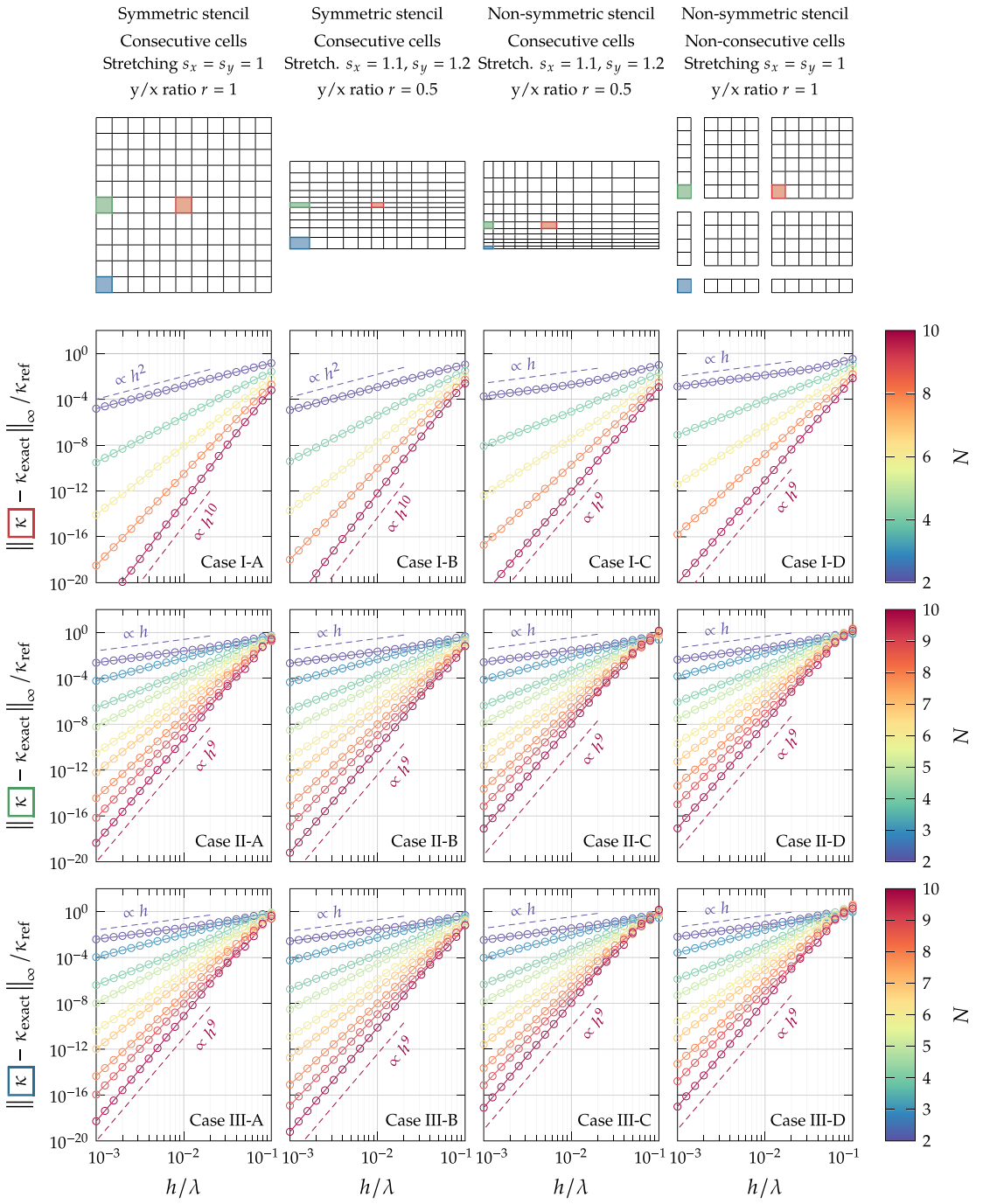

Fig. 7. Maximum errors associated with estimating the mean curvature of the test-surface in $N_S = 5 \times 10^5$ random configurations. Four different stencil types are considered, each corresponding to a column of the figure. The stencils are sketched at the top of the columns. The first row of graphs corresponds to the errors obtained in the central cell of the stencil, the second row to the errors obtained in the cell at the intersection of the left column and middle row of the stencil, and the third row to the errors in the bottom-left corner of the stencil. The use of $(N+1) \times (N+1)$ heights results in a curvature estimate of order $N-1$, unless the stencil is symmetric about its central x- and y-axis, in which case curvature can be estimated at its centre with order N.

For the three-dimensional study (Fig. 7), the following types of stencils are considered:

A Symmetric stencil formed by $N+1$ consecutive intervals of uniform width along both the x'- and y'-axis.

B Symmetric stencil formed by $N+1$ consecutive intervals of non-uniform width along both the x'- and y'-axis (the intervals are stretched by a factor $s_x = 1.1$ in the x' direction, and by a factor $s_y = 1.2$ in the y' direction). The ratio between the widths of the y' and x' intervals is $r = 0.5$.

C Non-symmetric stencil formed by $N+1$ consecutive intervals of non-uniform width along both the x'- and y'-axis (the intervals are stretched by a factor $s_x = 1.1$ in the positive x' direction, and by a factor $s_y = 1.2$ in the positive y' direction). The ratio between the widths of the y' and x' intervals is $r = 0.5$.
D Non-symmetric stencil formed by $N+1$ non-consecutive intervals of uniform width along both the x'- and y'-axis.

Curvature (and the associated error) is computed in:

I The central cell of the stencil (for N even).
II The cell at the intersection between the extreme left column and middle row of the stencil.
III The cell in the bottom left corner of the stencil.

These stencils are sketched above each column of Figs. 6 and 7. The intervals/cells in which curvature is estimated are highlighted on the stencil in red (central cell), green (left cell), and blue (corner cell). The errors are normalised with respect to κ_{ref}, the mean curvature of the surface at the centre of the domain, *i.e.* for $x = y = 0$. The width h of the cell under consideration is chosen as to yield h/λ ratios between 10^{-3} and 10^{-1}. For each value of h, $N_S = 5 \times 10^5$ curvature evaluations are conducted, each corresponding to a cell centre randomly chosen in $\mathcal{D}_{2\text{d}}$ or $\mathcal{D}_{3\text{d}}$, and each associated with a random value of θ, the angle of the rotation of $\mathcal{R}'$ relatively to $\mathcal{R}$. Values of N between 2 and 10 are considered for this study, resulting in a maximum possible order of convergence equal to 10. Finally, the coefficients $\lambda = 1$ and $\eta = 2/3$ are chosen.

From a computational point of view, all calculations are conducted in quadruple precision (128 bits) in order to not be limited by floating-point errors for the range of resolutions considered. The heights are integrated using the Gauss-Legendre quadrature rule with enough integration points so that no significant bias is introduced in the convergence study. The linear systems in Eqs. (15) and (25) are solved using LU decomposition.

Fig. 6 confirms that curvature can be estimated with a minimum order of accuracy $N-1$ anywhere in a stencil of $N+1$ (not necessarily consecutive) intervals of non-uniform width. If the stencil is symmetric about its centre, then curvature can be estimated with order N. Fig. 7 shows similar results for the three-dimensional case, *i.e.* that curvature can be estimated with a minimum order of accuracy $N-1$ anywhere in a stencil of $(N+1) \times (N+1)$ (not necessarily consecutive) domains of non-uniform dimensions. If the stencil is symmetric about its central x- and y-axis, then curvature can be estimated with order N.

Note that in the context of interfacial flow modelling, it is common to be unable to produce $N+1$ (in 2d) or $(N+1) \times (N+1)$ (in 3d) well-defined (or *consistent*) consecutive heights around a given cell [13]. This may, for instance, be due to the cell being close to a wall or domain boundary, to the interface being locally very curved, or to the interface topology being locally that of a thin film. The ability of the proposed approach to estimate curvature anywhere in a stencil of heights, as well as in stencils that are not made of consecutive heights, may prove useful when dealing with such configurations.

4.2. Comparison between second-order accurate formulations

On uniform Cartesian grids, in two dimensions, the approach proposed in this paper yields the exact same formulas for the second-order estimation of H_x and H_{xx} as those commonly used in the literature [10]. In the three-dimensional case, however, the coefficients resulting from the proposed approach, given in Eqs. (A.8), differ from those commonly found in the literature [11], given in Eqs. (22). Both formulations result in a second-order accurate estimation of curvature, but they produce different estimates of curvature and therefore different absolute errors.

The classical second-order central-difference formulas can actually be recovered from the fitting of a quadratic bivariate polynomial,

$$z = \tilde{f}(x, y) = ax^2 + bxy + cy^2 + dx + ey + g\,, \tag{30}$$

as opposed to the bivariate polynomial surface defined in Eq. (23). Such a polynomial surface, however, is characterised by only six scalar coefficients, meaning that the direct fitting of the surface onto the nine heights available in a 3×3 stencil results in an overdetermined equation system. The fitting problem thus needs to be reformulated into the following form,

$$\begin{cases} \tilde{H}_{i,j} = H_{i,j}\,, \quad \forall (i,j) \in \{-1,0,1\} \,|\, ij = 0\,, \\ \tilde{H}_{1,1} + \tilde{H}_{-1,-1} - \tilde{H}_{1,-1} - \tilde{H}_{-1,1} = H_{1,1} + H_{-1,-1} - H_{1,-1} - H_{-1,1}\,, \end{cases} \tag{$\mathcal{P}$}$$

that allows to uniquely recover the six scalar coefficients. The first five equations in ($\mathcal{P}$) uniquely determine the coefficients a, c, d, e, and g. The sixth equation in ($\mathcal{P}$) can be understood as a way to approximate the mixed second derivative of the surface height-function, therefore determining the coefficient b. Note that the coefficient b resulting from the solution of ($\mathcal{P}$) can also be recovered by averaging the coefficients resulting from the solution of the four fitting problems ($\mathcal{P}_{k,l}$)

$$\begin{cases} \tilde{H}_{i,j} = H_{i,j}\,, \quad \forall (i,j) \in \{-1,0,1\} \,|\, ij = 0\,, \\ \tilde{H}_{k,l} = H_{k,l}\,, \end{cases} \tag{$\mathcal{P}_{k,l}$}$$

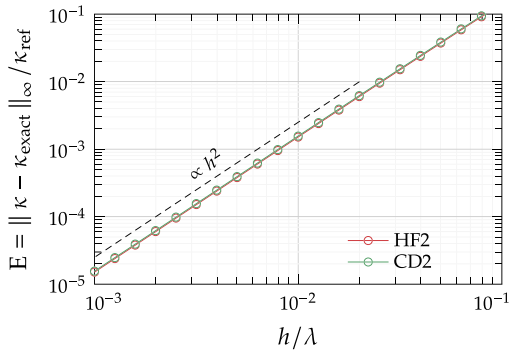

(a) Errors associated with the proposed (*HF2*) and classical central-difference (*CD2*) 2nd-order formulations, as a function of the ratio between the mesh spacing h and the length-scale λ

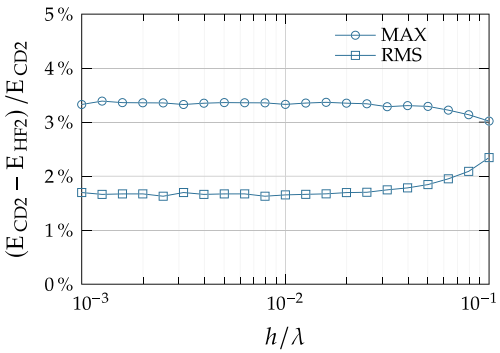

(b) Relative difference between the errors associated with the proposed (*HF2*) and classical central-difference (*CD2*) 2nd-order formulations, as a function of the ratio between the mesh spacing h and the length-scale λ

Fig. 8. Comparison between the errors obtained with the proposed second-order formulation (*HF2*) and the second-order formulation classically found in the litterature (*CD2*).

with $(k, l) \in \{-1, 1\}^2$. The fitting problem ($\mathcal{P}$) thus uniquely determines the six coefficients of the quadratic bivariate polynomial from the nine available heights, while retaining symmetry. The resulting formulas for the first and second partial derivatives are then those commonly found in the literature (Eqs. (22)).

The maximum errors associated with the formulas proposed in this paper (given in Eqs. (A.8) and referred to as *HF2*) and those found in the literature (given in Eqs. (22) and referred to as *CD2*), for the test-case described in Section 4, are shown in Fig. 8a. The relative differences between the maximum and root mean square errors associated with both methods are shown in Fig. 8b. These show that for the $N_S = 5 \times 10^5$ random configurations considered in the study, the maximum and root mean square errors associated with the proposed formulation (*HF2*) are approximately 3 % and 1 % smaller, respectively, than those associated with the classical formulation (*CD2*) – a difference that bears no major significance.

5. Conclusions

We have proposed a height-function method for the estimation of the local curvature on two- and three-dimensional non-uniform Cartesian grids, with arbitrary order of accuracy. The method relies upon the fitting of polynomial height-functions onto the heights of the discrete indicator function computed on the grid. The estimation of curvature at any arbitrary location of a non-uniform grid, and with arbitrary order, requires to solve a linear system for the coefficients of the polynomial height-function. This results in estimates of curvature that are of order $N - 1$ if $(N + 1)^{d-1}$ heights are available on a d-dimensional non-uniform grid. These estimates are of order N at the centre of the stencil if it is symmetric about its main central axis. This was confirmed by a comprehensive convergence analysis on the errors associated with the estimation of the local curvature of a fabricated test-curve and of a fabricated test-surface.

In the context of interfacial flow modelling, previous studies have shown that an increase in the order of accuracy of the curvature estimation can lead to an improved prediction of the interface dynamics, even when using a flow solver of lower order [12,2]. The method presented in this paper is thus expected to allow to tailor curvature estimation to the needs of the user and characteristics of the numerical framework employed. Moreover, recent work on the design of higher (than first) order surface tension models points towards the need for high-order representations of the fluid-fluid interface [20].

Finally, it should be mentioned that the fitting problems defined for the d-dimensional cases can be generalised to unstructured meshes, as done by the authors for the two-dimensional case [19]. The recovery of a curvature estimate of order $N - 1$ can thus be expected if $(N + 1)^{d-1}$ interfacial cells are used. The polynomial fitting problems, however, become non-linear and therefore need to be solved iteratively.

Declaration of competing interest

The authors declare that they have no known competing financial interests or personal relationships that could have appeared to influence the work reported in this paper.

Acknowledgements

This research was funded by the Deutsche Forschungsgemeinschaft (DFG, German Research Foundation), grant number 420239128.

Appendix A. Low-order formulas on uniform Cartesian grids

For conciseness, this appendix only considers the estimation of curvature on uniform Cartesian grids (up to 4th-order). Equivalent formulas for non-uniform Cartesian grids are considerably lengthier, which is why we recommend to use the general algorithms provided in Appendix B for such cases.

A.1. Two-dimensional case

The curvature at a given point on the curve is given by [9]

$$\kappa = \frac{H_{xx}}{\left(H_x^2 + 1\right)^{3/2}} \,. \tag{A.1}$$

A.1.1. Central cell

Consider the following stencil of consecutive intervals of uniform width h. Curvature is estimated at the centre of the cell with index 0, represented by the red dot.

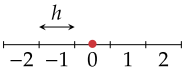

A 2nd-order accurate estimate of curvature at the highlighted coordinate can be obtained using

$$H_x = \frac{-H_{-1} + H_1}{2\,h} \,, \tag{A.2a}$$

$$H_{xx} = \frac{H_{-1} - 2\,H_0 + H_1}{h^2} \,. \tag{A.2b}$$

A 4th-order accurate estimate of curvature at the highlighted coordinate can be obtained using

$$H_x = \frac{5\,H_{-2} - 34\,H_{-1} + 34\,H_1 - 5\,H_2}{48\,h} \tag{A.3a}$$

$$H_{xx} = \frac{-H_{-2} + 12\,H_{-1} - 22\,H_0 + 12\,H_1 - H_2}{8\,h^2} \tag{A.3b}$$

A.1.2. Boundary cell

Consider the same stencil, in which curvature is now estimated at the centre of the extreme left cell.

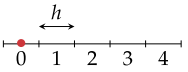

A 1st-order accurate estimate of curvature at the highlighted coordinate can be obtained using

$$H_x = \frac{-3\,H_0 + 4\,H_1 + -H_2}{2\,h} \tag{A.4a}$$

$$H_{xx} = \frac{H_0 - 2\,H_1 + H_2}{h^2} \tag{A.4b}$$

A 2nd-order accurate estimate of curvature at the highlighted coordinate can be obtained using

$$H_x = \frac{-43\,H_0 + 69\,H_1 - 33\,H_2 + 7\,H_3}{24\,h} \tag{A.5a}$$

$$H_{xx} = \frac{2\,H_0 - 5\,H_1 + 4\,H_2 - H_3}{h^2} \tag{A.5b}$$

A 3rd-order accurate estimate of curvature at the highlighted coordinate can be obtained using

$$H_x = \frac{-95\,H_0 + 174\,H_1 - 120\,H_2 + 50\,H_3 - 9\,H_4}{48\,h} \tag{A.6a}$$

$$H_{xx} = \frac{23\,H_0 - 68\,H_1 + 74\,H_2 - 36\,H_3 + 7\,H_4}{8\,h^2} \tag{A.6b}$$

A.2. Three-dimensional case

The mean curvature at a given point on the surface is given by

$$\kappa = \frac{H_{xx}\left(1+H_y^2\right) + H_{yy}\left(1+H_x^2\right) - 2\,H_x\,H_y\,H_{xy}}{\left(H_x^2+H_y^2+1\right)^{3/2}}\,. \tag{A.7}$$

A.2.1. Central cell

Consider the following stencil of consecutive x- and y-intervals of uniform width h and rh, respectively. Curvature is estimated at the centre of the cell with indices $(0,0)$, represented by the red dot.

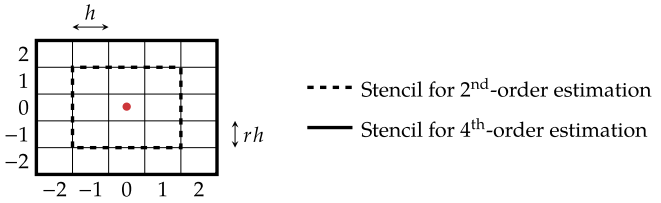

A 2nd-order accurate estimate of curvature at the highlighted coordinate can be obtained using

$$H_x = \frac{H_{-1,-1} - H_{1,-1} - 26\,H_{-1,0} + 26\,H_{1,0} + H_{-1,1} - H_{1,1}}{48\,h} \tag{A.8a}$$

$$H_y = \frac{H_{-1,-1} - H_{-1,1} - 26\,H_{0,-1} + 26\,H_{0,1} + H_{1,-1} - H_{1,1}}{48\,rh} \tag{A.8b}$$

$$H_{xx} = \frac{-H_{-1,-1} + 2\,H_{0,-1} - H_{1,-1} + 26\,H_{-1,0} - 52\,H_{0,0} + 26\,H_{1,0} - H_{-1,1} + 2\,H_{0,1} - H_{1,1}}{24\,h^2} \tag{A.8c}$$

$$H_{yy} = \frac{-H_{-1,-1} + 2\,H_{-1,0} - H_{-1,1} + 26\,H_{0,-1} - 52\,H_{0,0} + 26\,H_{0,1} - H_{1,-1} + 2\,H_{1,0} - H_{1,1}}{24\,(rh)^2} \tag{A.8d}$$

$$H_{xy} = \frac{H_{-1,-1} - H_{1,-1} - H_{-1,1} + H_{1,1}}{4\,rh^2} \tag{A.8e}$$

A 4th-order accurate estimate of curvature at the highlighted coordinate can be obtained using

$$H_x = \frac{\begin{array}{c}45\,H_{-2,-2} - 580\,H_{-2,-1} + 10670\,H_{-2,0} - 580\,H_{-2,1} + 45\,H_{-2,2} - 306\,H_{-1,-2} + 3944\,H_{-1,-1}\\ -72556\,H_{-1,0} + 3944\,H_{-1,1} - 306\,H_{-1,2} + 306\,H_{1,-2} - 3944\,H_{1,-1} + 72556\,H_{1,0}\\ -3944\,H_{1,1} + 306\,H_{1,2} - 45\,H_{2,-2} + 580\,H_{2,-1} - 10670\,H_{2,0} + 580\,H_{2,1} - 45\,H_{2,2}\end{array}}{92160\,h} \tag{A.9a}$$

$$H_y = \frac{\begin{array}{c}45\,H_{-2,-2} - 306\,H_{-2,-1} + 306\,H_{-2,1} - 45\,H_{-2,2} - 580\,H_{-1,-2} + 3944\,H_{-1,-1} - 3944\,H_{-1,1}\\ +580\,H_{-1,2} + 10670\,H_{0,-2} - 72556\,H_{0,-1} + 72556\,H_{0,1} - 10670\,H_{0,2} - 580\,H_{1,-2}\\ +3944\,H_{1,-1} - 3944\,H_{1,1} + 580\,H_{1,2} + 45\,H_{2,-2} - 306\,H_{2,-1} + 306\,H_{2,1} - 45\,H_{2,2}\end{array}}{92160\,rh} \tag{A.9b}$$

$$H_{xx} = \frac{\begin{array}{c}25608\,H_{-1,0} - 198\,H_{0,-2} + 2552\,H_{0,-1} - 9\,H_{-2,-2} + 116\,H_{-2,-1} + 116\,H_{-2,1} - 9\,H_{-2,2} + 108\,H_{-1,-2}\\ -1392\,H_{-1,-1} - 1392\,H_{-1,1} + 108\,H_{-1,2} + 25608\,H_{1,0} - 2134\,H_{2,0} + 2552\,H_{0,1} + 108\,H_{1,-2} - 1392\,H_{1,-1}\\ -1392\,H_{1,1} + 108\,H_{1,2} - 9\,H_{2,-2} - 2134\,H_{-2,0} - 46948\,H_{0,0} - 198\,H_{0,2} + 116\,H_{2,-1} + 116\,H_{2,1} - 9\,H_{2,2}\end{array}}{15360\,h^2} \tag{A.9c}$$

$$H_{yy} = \frac{\begin{array}{c}2552\,H_{-1,0} - 2134\,H_{0,-2} + 25608\,H_{0,-1} - 9\,H_{-2,-2} + 108\,H_{-2,-1} + 108\,H_{-2,1} - 9\,H_{-2,2} + 116\,H_{-1,-2}\\ -1392\,H_{-1,-1} - 1392\,H_{-1,1} + 116\,H_{-1,2} + 2552\,H_{1,0} - 198\,H_{2,0} + 25608\,H_{0,1} + 116\,H_{1,-2} - 1392\,H_{1,-1}\\ -1392\,H_{1,1} + 116\,H_{1,2} - 9\,H_{2,-2} - 198\,H_{-2,0} - 46948\,H_{0,0} - 2134\,H_{0,2} + 108\,H_{2,-1} + 108\,H_{2,1} - 9\,H_{2,2}\end{array}}{15360\,(rh)^2} \tag{A.9d}$$

$$H_{xy} = \frac{\begin{array}{c}25\,H_{-2,-2} - 170\,H_{-2,-1} + 170\,H_{-2,1} - 25\,H_{-2,2} - 170\,H_{-1,-2} + 1156\,H_{-1,-1} - 1156\,H_{-1,1} + 170\,H_{-1,2}\\ +170\,H_{1,-2} - 1156\,H_{1,-1} + 1156\,H_{1,1} - 170\,H_{1,2} - 25\,H_{2,-2} + 170\,H_{2,-1} - 170\,H_{2,1} + 25\,H_{2,2}\end{array}}{2304\,rh^2} \tag{A.9e}$$

A.2.2. Boundary cell

Consider the following stencil of consecutive x- and y-intervals of uniform width h and rh, respectively. Curvature is estimated at the centre of the cell with indices $(0, 0)$, represented by the red dot.

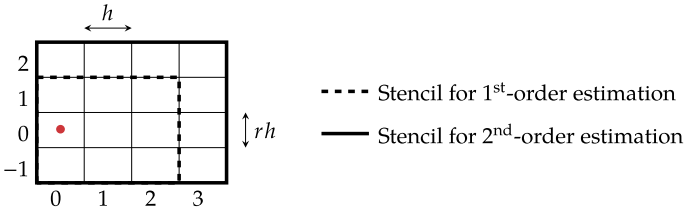

A 1st-order accurate estimate of curvature at the highlighted coordinate can be obtained using

$$H_x = \frac{3\,H_{0,-1} - 4\,H_{1,-1} + H_{2,-1} - 78\,H_{0,0} + 104\,H_{1,0} - 26\,H_{2,0} + 3\,H_{0,1} - 4\,H_{1,1} + H_{2,1}}{48\,h} \tag{A.10a}$$

$$H_y = \frac{-23\,H_{0,-1} - 2\,H_{1,-1} + H_{2,-1} + 23\,H_{0,1} + 2\,H_{1,1} - H_{2,1}}{48\,rh} \tag{A.10b}$$

$$H_{xx} = \frac{-H_{0,-1} + 2\,H_{1,-1} - H_{2,-1} + 26\,H_{0,0} - 52\,H_{1,0} + 26\,H_{2,0} - H_{0,1} + 2\,H_{1,1} - H_{2,1}}{24\,h^2} \tag{A.10c}$$

$$H_{yy} = \frac{23\,H_{0,-1} + 2\,H_{1,-1} - H_{2,-1} - 46\,H_{0,0} - 4\,H_{1,0} + 2\,H_{2,0} + 23\,H_{0,1} + 2\,H_{1,1} - H_{2,1}}{24\,(rh)^2} \tag{A.10d}$$

$$H_{xy} = \frac{3\,H_{0,-1} - 4\,H_{1,-1} + H_{2,-1} - 3\,H_{0,1} + 4\,H_{1,1} - H_{2,1}}{4\,rh^2} \tag{A.10e}$$

A 2nd-order accurate estimation of curvature at the highlighted coordinate can be obtained using

$$H_x = \frac{\begin{array}{r}43\,H_{0,-1} - 1118\,H_{0,0} + 43\,H_{0,1} - 69\,H_{1,-1} + 1794\,H_{1,0} - 69\,H_{1,1} \\ +33\,H_{2,-1} - 858\,H_{2,0} + 33\,H_{2,1} - 7\,H_{3,-1} + 182\,H_{3,0} - 7\,H_{3,1}\end{array}}{576\,h} \tag{A.11a}$$

$$H_y = \frac{\begin{array}{r}-154\,H_{0,-1} - 330\,H_{0,0} + 594\,H_{0,1} - 110\,H_{0,2} - 35\,H_{1,-1} - 75\,H_{1,0} + 135\,H_{1,1} - 25\,H_{1,2} \\ +28\,H_{2,-1} + 60\,H_{2,0} - 108\,H_{2,1} + 20\,H_{2,2} - 7\,H_{3,-1} - 15\,H_{3,0} + 27\,H_{3,1} - 5\,H_{3,2}\end{array}}{576\,rh} \tag{A.11b}$$

$$H_{xx} = \frac{\begin{array}{r}-2\,H_{0,-1} + 52\,H_{0,0} - 2\,H_{0,1} + 5\,H_{1,-1} - 130\,H_{1,0} + 5\,H_{1,1} \\ -4\,H_{2,-1} + 104\,H_{2,0} - 4\,H_{2,1} + H_{3,-1} - 26\,H_{3,0} + H_{3,1}\end{array}}{24\,h^2} \tag{A.11c}$$

$$H_{yy} = \frac{\begin{array}{r}22\,H_{0,-1} - 44\,H_{0,0} + 22\,H_{0,1} + 5\,H_{1,-1} - 10\,H_{1,0} + 5\,H_{1,1} \\ -4\,H_{2,-1} + 8\,H_{2,0} - 4\,H_{2,1} + H_{3,-1} - 2\,H_{3,0} + H_{3,1}\end{array}}{24\,(rh)^2} \tag{A.11d}$$

$$H_{xy} = \frac{\begin{array}{r}301\,H_{0,-1} + 645\,H_{0,0} - 1161\,H_{0,1} + 215\,H_{0,2} - 483\,H_{1,-1} - 1035\,H_{1,0} + 1863\,H_{1,1} - 345\,H_{1,2} \\ +231\,H_{2,-1} + 495\,H_{2,0} - 891\,H_{2,1} + 165\,H_{2,2} - 49\,H_{3,-1} - 105\,H_{3,0} + 189\,H_{3,1} - 35\,H_{3,2}\end{array}}{576\,rh^2} \tag{A.11e}$$

A.2.3. Corner cell

Consider the following stencil of consecutive x- and y-intervals of uniform width h and rh, respectively. Curvature is estimated at the centre of the cell with indices $(0, 0)$, represented by the red dot.

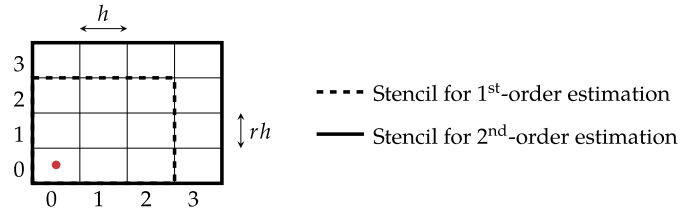

A 1st-order accurate estimate of curvature at the highlighted coordinate can be obtained using

$$H_x = \frac{-69\,H_{0,0} + 92\,H_{1,0} - 23\,H_{2,0} - 6\,H_{0,1} + 8\,H_{1,1} - 2\,H_{2,1} + 3\,H_{0,2} - 4\,H_{1,2} + H_{2,2}}{48\,h} \tag{A.12a}$$

$$H_y = \frac{-69\,H_{0,0} - 6\,H_{1,0} + 3\,H_{2,0} + 92\,H_{0,1} + 8\,H_{1,1} - 4\,H_{2,1} - 23\,H_{0,2} - 2\,H_{1,2} + H_{2,2}}{48\,rh} \tag{A.12b}$$

$$H_{xx} = \frac{23\,H_{0,0} - 46\,H_{1,0} + 23\,H_{2,0} + 2\,H_{0,1} - 4\,H_{1,1} + 2\,H_{2,1} - H_{0,2} + 2\,H_{1,2} - H_{2,2}}{24\,h^2} \tag{A.12c}$$

$$H_{yy} = \frac{23\,H_{0,0} + 2\,H_{1,0} - H_{2,0} - 46\,H_{0,1} - 4\,H_{1,1} + 2\,H_{2,1} + 23\,H_{0,2} + 2\,H_{1,2} - H_{2,2}}{24\,(rh)^2} \tag{A.12d}$$

$$H_{xy} = \frac{9\,H_{0,0} - 12\,H_{1,0} + 3\,H_{2,0} - 12\,H_{0,1} + 16\,H_{1,1} - 4\,H_{2,1} + 3\,H_{0,2} - 4\,H_{1,2} + H_{2,2}}{4\,rh^2} \tag{A.12e}$$

A 2nd-order accurate estimate of curvature at the highlighted coordinate can be obtained using

$$H_x = \frac{\begin{array}{r}-946\,H_{0,0} - 215\,H_{0,1} + 172\,H_{0,2} - 43\,H_{0,3} + 1518\,H_{1,0} + 345\,H_{1,1} - 276\,H_{1,2} + 69\,H_{1,3}\\ -726\,H_{2,0} - 165\,H_{2,1} + 132\,H_{2,2} - 33\,H_{2,3} + 154\,H_{3,0} + 35\,H_{3,1} - 28\,H_{3,2} + 7\,H_{3,3}\end{array}}{576\,h} \tag{A.13a}$$

$$H_y = \frac{\begin{array}{r}-946\,H_{0,0} + 1518\,H_{0,1} - 726\,H_{0,2} + 154\,H_{0,3} - 215\,H_{1,0} + 345\,H_{1,1} - 165\,H_{1,2} + 35\,H_{1,3}\\ +172\,H_{2,0} - 276\,H_{2,1} + 132\,H_{2,2} - 28\,H_{2,3} - 43\,H_{3,0} + 69\,H_{3,1} - 33\,H_{3,2} + 7\,H_{3,3}\end{array}}{576\,rh} \tag{A.13b}$$

$$H_{xx} = \frac{\begin{array}{r}44\,H_{0,0} + 10\,H_{0,1} - 8\,H_{0,2} + 2\,H_{0,3} - 110\,H_{1,0} - 25\,H_{1,1} + 20\,H_{1,2} - 5\,H_{1,3}\\ +88\,H_{2,0} + 20\,H_{2,1} - 16\,H_{2,2} + 4\,H_{2,3} - 22\,H_{3,0} - 5\,H_{3,1} + 4\,H_{3,2} - H_{3,3}\end{array}}{24\,h^2} \tag{A.13c}$$

$$H_{yy} = \frac{\begin{array}{r}44\,H_{0,0} - 110\,H_{0,1} + 88\,H_{0,2} - 22\,H_{0,3} + 10\,H_{1,0} - 25\,H_{1,1} + 20\,H_{1,2} - 5\,H_{1,3}\\ -8\,H_{2,0} + 20\,H_{2,1} - 16\,H_{2,2} + 4\,H_{2,3} + 2\,H_{3,0} - 5\,H_{3,1} + 4\,H_{3,2} - H_{3,3}\end{array}}{24\,(rh)^2} \tag{A.13d}$$

$$H_{xy} = \frac{\begin{array}{r}1849\,H_{0,0} - 2967\,H_{0,1} + 1419\,H_{0,2} - 301\,H_{0,3} - 2967\,H_{1,0} + 4761\,H_{1,1} - 2277\,H_{1,2} + 483\,H_{1,3}\\ +1419\,H_{2,0} - 2277\,H_{2,1} + 1089\,H_{2,2} - 231\,H_{2,3} - 301\,H_{3,0} + 483\,H_{3,1} - 231\,H_{3,2} + 49\,H_{3,3}\end{array}}{576\,rh^2} \tag{A.13e}$$

Appendix B. C implementations

B.1. Two-dimensional case

Listing 1: C code to estimate the curvature of a two-dimensional curve from $N+1$ heights.

```c
double TwoDCurvature(int N, double *H, double *xmin, double *xmax, double xc)
{
  /*        H: 1d array of size (N+1) containing the heights
   xmin, xmax: 1d arrays of size (N+1) containing the limits of the height intervals
           xc: coordinate at which curvature is to be estimated */

  int i, j;
  double M[N + 1][N + 1], A[N + 1];

  for (i = 0; i < N + 1; i++)
  {
    for (j = 0; j < N + 1; j++)
    {
      M[i][j] = (pow(xmax[i] - xc, (double) j + 1) - pow(xmin[i] - xc, (double) j + 1))
          / (((double) j + 1) * (xmax[i] - xmin[i]));
    }
  }

  Solve(M, A, H);  /* Returns A = inv(M) H (using LU decomposition, for instance) */

  return 2.0 * A[2] / pow(1.0 + A[1] * A[1], 1.5);
}
```

B.2. Three-dimensional case

Listing 2: C code to estimate the mean curvature of a three-dimensional surface from $(N+1) \times (N+1)$ heights.

```c
double ThreeDCurvature(int N, double **H, double *xmin, double *xmax, double *ymin, double *ymax,
    double xc, double yc)
{
  /*        H: 2d array of size (N+1)x(N+1) containing the heights
   xmin, xmax: 1d arrays of size (N+1) containing the x-limits of the height domains
   ymin, ymax: 1d arrays of size (N+1) containing the y-limits of the height domains
       xc, yc: coordinates at which curvature is to be estimated */

  int i, j, m, n;
  double M[(N + 1) * (N + 1)][(N + 1) * (N + 1)], A[(N + 1) * (N + 1)], Hvec[(N + 1) * (N + 1)];

  for (j = 0; j < N + 1; j++)
  {
    for (i = 0; i < N + 1; i++)
    {
      Hvec[i + j * (N + 1)] = H[i][j];

      for (n = 0; n < N + 1; n++)
      {
        for (m = 0; m < N + 1; m++)
        {
          M[i + j * (N + 1)][m + n * (N + 1)] =
              (pow(xmax[i] - xc, (double) m + 1) - pow(xmin[i] - xc, (double) m + 1))
              * (pow(ymax[j] - yc, (double) n + 1) - pow(ymin[j] - yc, (double) n + 1))
              / (((double) m + 1) * ((double) n + 1) * (xmax[i] - xmin[i]) * (ymax[j] - ymin[j]));
        }
      }
    }
  }

  Solve(M, A, Hvec); /* Returns A = inv(M) Hvec (using LU decomposition, for instance) */

  return 2.0 * (A[2] * (1.0 + A[N + 1] * A[N + 1]) + A[2 * N + 2] * (1.0 + A[1] * A[1]) - A[N + 2] * A[1]
      * A[N + 1]) / pow(1.0 + A[1] * A[1] + A[N + 1] * A[N + 1], 1.5);
}
```

References

[1] T. Abadie, J. Aubin, D. Legendre, On the combined effects of surface tension force calculation and interface advection on spurious currents within volume of fluid and level set frameworks, J. Comput. Phys. 297 (2015) 611–636.
[2] M. Coquerelle, S. Glockner, A fourth-order accurate curvature computation in a level set framework for two-phase flows subjected to surface tension forces, J. Comput. Phys. 305 (2016) 838–876.
[3] S. Popinet, Numerical models of surface tension, Annu. Rev. Fluid Mech. 50 (2018) 49–75.
[4] R.B. DeBar, Fundamentals of the KRAKEN Code: Eulerian Hydrodynamics Code for Compressible Nonviscous Flow of Several Fluids in Two-Dimensional (Axially Symmetric) Region, Technical Report, California University, Livermore (USA), Lawrence Livermore Lab, 1974.
[5] W.F. Noh, P. Woodward, SLIC (Simple Line Interface Calculation), in: A.I. van de Vooren, P.J. Zandbergen (Eds.), Proceedings of the Fifth International Conference on Numerical Methods in Fluid Dynamics, June 28–July 2, 1976, Twente University, Enschede, in: Lecture Notes in Physics, Springer, Berlin, Heidelberg, 1976, pp. 330–340.
[6] C. Hirt, B. Nichols, Volume of fluid (VOF) method for the dynamics of free boundaries, J. Comput. Phys. 39 (1981) 201–225.
[7] W.J. Rider, D.B. Kothe, Reconstructing volume tracking, J. Comput. Phys. 141 (1998) 112–152.
[8] R. Scardovelli, S. Zaleski, Direct numerical simulation of free-surface and interfacial flow, Annu. Rev. Fluid Mech. 31 (1999) 567–603.
[9] R. Goldman, Curvature formulas for implicit curves and surfaces, Comput. Aided Geom. Des. 22 (2005) 632–658.
[10] S. Cummins, M. Francois, D. Kothe, Estimating curvature from volume fractions, Comput. Struct. 83 (2005) 425–434.
[11] M. Francois, S. Cummins, E. Dendy, D. Kothe, J. Sicilian, M. Williams, A balanced-force algorithm for continuous and sharp interfacial surface tension models within a volume tracking framework, J. Comput. Phys. 213 (2006) 141–173.
[12] M. Sussman, M. Ohta, High-order techniques for calculating surface tension forces, in: I.N. Figueiredo, J.F. Rodrigues, L. Santos (Eds.), Free Boundary Problems: Theory and Applications, Birkhäuser Basel, Basel, 2007, pp. 425–434.
[13] S. Popinet, An accurate adaptive solver for surface-tension-driven interfacial flows, J. Comput. Phys. 228 (2009) 5838–5866.
[14] M. Owkes, O. Desjardins, A computational framework for conservative, three-dimensional, unsplit, geometric transport with application to the volume-of-fluid (VOF) method, J. Comput. Phys. 270 (2014) 587–612.
[15] C. Ivey, P. Moin, Accurate interface normal and curvature estimates on three-dimensional unstructured non-convex polyhedral meshes, J. Comput. Phys. 300 (2015) 365–386.
[16] M. Francois, B. Swartz, Interface curvature via volume fractions, heights, and mean values on nonuniform rectangular grids, J. Comput. Phys. 229 (2010) 527–540.
[17] G. Bornia, A. Cervone, S. Manservisi, R. Scardovelli, S. Zaleski, On the properties and limitations of the height function method in two-dimensional Cartesian geometry, J. Comput. Phys. 230 (2011) 851–862.
[18] Q. Zhang, HFES: a height function method with explicit input and signed output for high-order estimations of curvature and unit vectors of planar curves, SIAM J. Numer. Anal. 55 (2017) 1024–1056.
[19] F. Evrard, F. Denner, B. van Wachem, Estimation of curvature from volume fractions using parabolic reconstruction on two-dimensional unstructured meshes, J. Comput. Phys. 351 (2017) 271–294.
[20] M.O. Abu-Al-Saud, S. Popinet, H.A. Tchelepi, A conservative and well-balanced surface tension model, J. Comput. Phys. 371 (2018) 896–913.